Journal of Multidisciplinary Engineering Science and Technology (JMEST)
ISSN: 2458-9403
Vol. 8 Issue 10, October - 2021

KYAMOS Software – Brief Review of Lattice Boltzmann simulations

Antonis P. Papadakis, Aimilios Ioannou Andreas Georgiou and Wasif Almady
KYAMOS LTD, 37 Polyneikis Street, Strovolos, 2047, Nicosia, Cyprus

***Abstract*— In this paper, we present a review of the theory behind the Lattice Boltzmann method, utilized increasingly in the simulation of incompressible flows. The aim of this paper is to gather all the necessary data and be used as a guide and reference for anyone that wishes to apply the Lattice Boltzmann-Multiple Relaxation Time method (LB-MRT), well known for its stability, speed and accuracy. The paper includes all the necessary equations to build models both in two and three-dimensions and some of the obtained results are presented both for the standard LB-BGK and the LB-MRT method. Specifically, all the moment matrices and their inverses, as well as the equilibrium equations. To conclude, LB-MRT is a method well suited for parallelization, and when utilized on GPU, we can see fast speeds and benefits in running times and accuracy. We also discuss the treatment of boundary conditions and present a totalistic approach in treating inflow, no-slip, outflow or pressure boundary conditions. KYAMOS intends to release a proprietary software utilizing GPU-InfiniBand, cloud computing environment for the utilization of LB-MRT method in various fields of engineering and physics.**

Keywords—Lattice Boltzmann; Multiple Relaxation Time; incompressible flows;

I. INTRODUCTION

In this paper, we present the mathematical formulation of the Lattice Boltzmann, Multiple Relaxation Time method (LB-MRT). First, we provide an introduction on the Lattice Boltzmann method and the reason the MRT scheme has accumulated great attention. Then we present the limitations of the BGK method and the stability considerations solved by the MRT. Thereafter, we derive the MRT method mathematically, and present the various matrices which are necessary in conducting MRT simulations. This includes the transformation matrix M to revert from equilibrium distribution to moment space to conduct the collision step and the inverse transformation matrix M^{-1} to revert from the moment to equilibrium distribution space to conduct the streaming step. Stability issues are discussed and the matrices for various cases of two and three dimensions are listed, with an attempt for this manuscript to be used as a reference for anyone who wishes to conduct LB-MRT simulations. Finally, we present some results obtained with using the LB-BGK and LB-MRT methods running on the GPU, which shows the real advantages of utilizing incompressible Lattice Boltzmann simulations on the GPUs due to their inherent data locality and prawn to parallelization.

II. LITERATURE REVIEW OF MRT METHOD

Tubbs et al. [1] use the MRT method to simulate multilayer shallow water flows with graphics processing units. The use of multiple relaxation times enabled the authors to handle very low kinematic viscosity without causing a stability issues in the shallow water equations. They solve the multilayer Saint-Venant equations to obtain horizontal flow velocities in various depths, with good speedup and scalability for large problems.

Sato et al. [2] study free-surface flow problems that usually occur in numerous disaster simulations, such as tsunami inland penetration in urban areas. The authors stress the complexity in solving the pressure Poisson equation in incompressible Navier-Stokes fluid modeling in large scale in 3-dimensions, and present the lattice Boltzmann method, and specifically MRT collision model, along with the piecewise linear interface calculation (PLIC) approach. Through classic dam-break problems, they validate the appropriate parameter settings, including the weak compressibility, for tsunami simulations. The authors verify through benchmark tests that the method accurately simulates the three-dimensional dam-break flow and controls the compressibility drop in the second-order value of the Mach number.

Purqon [3] implements BGK and MRT Lattice Boltzmann solutions for incompressible two-dimensional lid-driven cavity. A stability analysis is performed by finding the maximum Reynolds number and velocity for the solution to converge. The velocity profile is compared with the benchmark results from Ghia, et al. and conclude that MRT is more stable than BGK, with a similar accuracy, with the maximum Reynolds number for convergence being 3,200 for BGK and 7,500 for MRT.

Yang et al. [4] study the flow pattern in a two-dimensional lid-driven semi-circular cavity using the MRT method by varying the Reynolds number from 5,000 to 50,000. It is shown that with the increase of the Re number, the flow experiences a complex transition (from steady to the periodic flow, and finally to the chaotic flow), with the MRT depicting superiority in numerical stability at high Reynolds number.

Bouarnouna et al. [5] study the laminar natural convection in a horizontal channel with porous blocks periodically distributed on its lower adiabatic surface

using the MRT method. The D2Q9 is used to solve the flow field, while the D2Q5 is used to solve for the temperature field. The Darcy number effect (10.1 ≤ Da ≤ 10.6), the Rayleigh number (103 ≤ Ra ≤ 107) and the relative porous blocks height (1/8 ≤ D ≤ 1/2) are varied, and the results obtained show the significance of the above parameters for both flow and heat transfer structures.

Chai et al. [6] present a unified framework of MRT method for the Navier-Stokes and non-linear convection-diffusion equations, where they introduce a block-lower-triangular-relaxation matrix and an auxiliary source distribution function. A direct comparison between Chapman-Enskog, Maxwell iteration, direct Taylor expansion, and recurrence equations techniques that are used show that they are able to recover the macroscopic Navier-Stokes and the non-linear convection-diffusion equations.

De Rosis et al. [7] propose a D3Q27 discretization, where the quantities relax towards an elegant Galilean invariant equilibrium by including the effect of external accelerations. In another later paper, they investigate the usage of the D3Q19 model [8], and the results are compared in terms of stability and accuracy on single, multi-phase, and magnetohydrodynamics flow simulations. It is shown that there is little impact on the accuracy and stability for moderate Reynolds number flows in the weakly compressible regime, when the D3Q19 is used.

Razzaghian et al. [9] study the lid driven cavity flow between MRT-D2Q9 and Single-relaxation-time (SRT-D2Q9) and compare them in terms of speed and stability with the Reynolds number ranging from 100 to 3,200 and show that the MRT produces more stable and accurate results than the SRT model.

Luo et al. [10] present a unified Lattice Boltzmann model that integrates the BGK, MRT, central-moment or cascaded lattice Boltzmann method and multiple entropic operators (KBC) methods. They analyze the relations between the above four operators and demonstrate the flexibility of the Unified LBM framework (ULBM) in three multiphase flow problems: (a) the rheology of an emulsion, (b) splashing of a droplet on a liquid film, and: (c) dynamics of pool boiling.

Jahanshaloo [11] et al. use the MRT model coupled with a Large Eddy Simulation (LES) to study the lid driven cavity flow at different Reynolds number (1,000-10,000) and the results are compared with other papers that solve the Navier stokes equation directly. The results show that the MRT with LES solves the complex flows with reasonable accuracy and reliability, when compared to traditional Navier-Stokes solutions.

Ammar et al. [12] propose a 3D MRT model for multiphase flows at large density ratios, with the model being capable of adjusting the surface tension independently of the density ratio, and the proposed scheme is validated by verifying Laplace's law and by analyzing its thermodynamic consistency and the oscillation period of a deformed droplet. Thereafter, it is used in the simulation of the impact of a droplet on a dry surface, where impact dynamics and maximum spread factor are calculated for different Reynolds and Weber numbers. Finally, they apply the model on the impact of a droplet on a wet surface and the propagation of transverse waves on the liquid surface are analyzed successfully.

III. Mathematical Formulation of MRT

A. *Introduction*

Since the invention of the Boltzmann equation in 1872, many attempts to find a proper mathematical expression for the collision term have been conducted. This was mainly due to complexities and difficulties to solve the collision term. A BGK model has been introduced to simplify the solution with low significant errors of the outcome of the Lattice Boltzmann equation, expressing the collision term as a linear relationship between the distribution function in the non-equilibrium state with its equilibrium state:

$$\Omega_i = -\frac{f_i - f_i^{eq}}{\tau} \quad (1)$$

The equation can be interpreted as the tendency of the non-equilibrium distribution function to relax to its equilibrium state after a time τ called relaxation time. It is a very simple mathematical expression to express the collision term, but at the cost of accuracy and stability.s

Multiple-relaxation-time (MRT) method has been introduced to solve the issues relating to the stability and accuracy, since it offers multiple relaxation times to be adjusted accordingly. The main difference between the BGK and the MRT methods is that the BGK contains one relaxation time τ for all the population of distribution functions, whereas the MRT uses different relaxations times τ for the population of distribution function, which leads to more freedom to adjust the relaxation time parameters to get more stability.

B. *Derivation of the MRT method*

One starts from the conversation of the mass where the following equation can be formulated:

$$\sum_i \Omega_i = -\sum_i \frac{f_i - f_i^{eq}}{\tau} \quad (2)$$

The $1/\tau$ can be expressed as ω and is called the relaxation rate. With the absent of the force, equation (1) can be written in the following form:

$$\sum_i \Omega_i = -\sum_i \omega \left(f_i - f_i^{eq}\right) = 0 \quad (3)$$

which leads to:

$$-\omega \left(\rho - \rho^{eq}\right) = 0 \quad (4)$$

where ρ represents the density of the zeroth velocity moment. From the conversation of the momentum, the following equations can be formulated:

$$\sum_i \Omega_i c_i = -\sum_i \omega \left(c_i f_i - c_i f_i^{eq}\right) = 0 \quad (5)$$

Equation (4) is converted into moment space:

$$-\omega \left(j - j^{eq}\right) = 0 \quad (6)$$

where j represents the momentum of the first order velocity. In equation (4) and (6), all the momentum zeroth order and first order velocity are relaxed with one relaxation rate ω. The main idea behind the MRT is to relax each moment with its relaxation rate to achieve better stability and accuracy. The MRT procedure is to map the collision term from the distribution space to the moment space, let them collide and then map the moment space back to distribution function, to perform the streaming step. To establish the mathematical steps in order to get the moment space, we will start from the fact that any function can be approximated by Taylor series or other polynomials.

The distribution function can be approximated by using Taylor series expansion:

$$e^x = 1 + x + \frac{x^2}{2!} + \frac{x^3}{3!} + \cdots \tag{7}$$

The distribution function is:

$$f = \frac{3\rho}{2\pi} e^{-\frac{3}{2(\xi-u)}^2} \tag{8}$$

where ρ is the density, the vector ξ represents the velocity of the particle and the vector u is the macroscopic velocity. Equation (8) can be written as follows:

$$f = \frac{3\rho}{2\pi} e^{-\frac{3\xi^2}{2}} e^{\frac{3(\xi.u-u^2)}{2}} \tag{9}$$

We can use Taylor series to expand the exponential that contains the macroscopic velocity and truncate the second order and above, to get:

$$f = \frac{3\rho}{2\pi} e^{-\frac{3\xi^2}{2}} \left[1 + \frac{3}{2}\xi.u - \frac{3}{2}u^2\right] \tag{10}$$

Hermite polynomial is a good choice to approximate the distribution function:

$$H^n = (-1)^n \left[\frac{1}{\sqrt{2\pi}} e^{-x^2}\right]^{-1} \frac{d^n}{dx^n}\left[\frac{1}{\sqrt{2\pi}} e^{-x^2}\right] \tag{11}$$

where H^n is Hermite polynomials and n is the order of this polynomial. Equation (11) can be written as:

$$H^n = (-1)^n [\omega]^{-1} \frac{d^n}{dx^n}[\omega] \tag{12}$$

where ω is the weight function. In three-dimensions, equation (12) can be written as:

$$H^n = (-1)^n [\omega(x,y,z)]^{-1} \nabla^n [\omega(x,y,z)] \tag{13}$$

where $\omega(x,y,z)$ is:

$$\omega(x,y,z) = \frac{1}{(2\pi)^{\frac{3}{2}}} e^{-(x^2+y^2+z^2)} \tag{14}$$

Hermite polynomials corresponds to orthogonality:

$$\int_{-\infty}^{\infty} \omega(x) H^n H^m \, dx = n!\, \delta_{mn} \tag{15}$$

where δ_{mn} is the Kronecker delta which is a function of two variables m and n, with the function being 1 when m and n are equal and 0 when m and n are not equal. Equation (15) can be extended to 3D:

$$\iiint_{-\infty}^{\infty} \omega(x,y,z) H_\alpha^m H_\beta^n dxdydz = n_x!\, n_y!\, n_z!\, \delta_{mn}\delta_{\alpha\beta} \tag{16}$$

where $\delta_{\alpha\beta}$ is 1 when α is the permutation of β. The distribution function can be approximated by using the Hermite polynomial as the basis functions multiplied by coefficients, a similar idea of the Fourier series:

$$f = \omega(x,y,z) \sum_{n=0}^{\infty} \frac{1}{n_x!\, n_y!\, n_z!} a^n . H^n \tag{17}$$

The coefficient a^n can be found by multiplying both sides with H^m and integrate both sides as follows:

$$\iiint_{-\infty}^{\infty} f H^m dxdydz = a^n \frac{1}{n_x!\, n_y!\, n_z!} \sum_{n=0}^{\infty} \iiint_{-\infty}^{\infty} \omega(x,y,z) H^n H^m dxdydz \tag{18}$$

It has a solution only when n equals m and α is the permutation of β. Then equation (18) becomes:

$$a^n = \iiint_{-\infty}^{\infty} f H^n dxdydz \tag{19}$$

We can assume the Hermite polynomial as a function of the velocity of the particles instead of the spatial dimensions:

$$H^n = (-1)^n \left[\omega(\xi_x, \xi_y, \xi_z)\right]^{-1} \nabla^n \left[\omega(\xi_x, \xi_y, \xi_z)\right] \tag{20}$$

and equation (19) becomes:

$$a^n = \iiint_{-\infty}^{\infty} f H^n d\xi_x d\xi_y d\,\xi_z \tag{21}$$

which leads to:

$$a^0 = \iiint_{-\infty}^{\infty} f H^0 d\xi_x d\xi_y d\,\xi_z \to a^0 = \iiint_{-\infty}^{\infty} f d\xi_x d\xi_y d\,\xi_z \to a^0 = \rho \tag{22}$$

$$a_x^1 = \iiint_{-\infty}^{\infty} f H_x^1 d\xi_x d\xi_y d\,\xi_z \to a_x^1 = \iiint_{-\infty}^{\infty} f \xi_x d\xi_x d\xi_y d\,\xi_z \to a_x^1 = \rho u_x \tag{23}$$

$$a_y^1 = \iiint_{-\infty}^{\infty} f H_y^1 d\xi_x d\xi_y d\,\xi_z \to a_x^1 = \iiint_{-\infty}^{\infty} f \xi_y d\xi_x d\xi_y d\,\xi_z \to a_y^1 = \rho u_y \tag{24}$$

$$a_z^1 = \iiint_{-\infty}^{\infty} f H_z^1 d\xi_x d\xi_y d\,\xi_z \to a_x^1 = \iiint_{-\infty}^{\infty} f \xi_z d\xi_x d\xi_y d\,\xi_z \to a_z^1 = \rho u_z \tag{25}$$

In the second order, there will be 9 configurations while in the third order, there will be 27 configurations. If we take a deep look at the resulting coefficients, we will find out that the coefficient of the Hermit polynomial equals the conserved moments, with zeroth order of the coefficient (zero order velocity) being the density, first order of coefficient being the first order moment etc.

Hence, equation (21) can be discretized as follows:

$$a^n = \sum_i H_i^n f_i \tag{26}$$

where the coefficient a^n with m_j represents the conserved moments, the H_i^n with M_i^j represents a matrix $j \times i$. Equation (21) can be written as follows:

$$m_j = \sum_{i=0}^{j} M_i^j f_i \quad (27)$$

Equation (27) can be written in vector-matrix form:

$$m = Mf \quad (28)$$

If we have D3Q19, equation (28) becomes:

$$\begin{pmatrix} m_0 \\ \vdots \\ m_{18} \end{pmatrix} = \begin{pmatrix} M_0^0 \cdots M_{18}^0 \\ \vdots \quad \vdots \quad \vdots \\ M_0^{18} \cdots M_{18}^{18} \end{pmatrix} \begin{pmatrix} f_0 \\ \vdots \\ f_{18} \end{pmatrix} \quad (29)$$

If we reconstruct the Lattice Boltzmann equation in discretized vector form:

$$f(x + c_x\Delta t, y + c_y\Delta t, z + c_z\Delta t, t + \Delta t) - f(x, y, z, t) = -\omega\,(f - f^{eq}) \quad (30)$$

we can create the matrix M in equation (30) as follows:

$$f(x + c_x\Delta t, y + c_y\Delta t, z + c_z\Delta t, t + \Delta t) - f(x, y, z, t) = -M^{-1}M\,\omega\,(f - f^{eq}) \quad (31)$$

which leads to:

$$f(x + c_x\Delta t, y + c_y\Delta t, z + c_z\Delta t, t + \Delta t) - f(x, y, z, t) = -M^{-1}\omega I\,(Mf - Mf^{eq}) \quad (32)$$

which leads to:

$$f(x + c_x\Delta t, y + c_y\Delta t, z + c_z\Delta t, t + \Delta t) - f(x, y, z, t) = -M^{-1}\,\mathrm{S}(m - m^{eq}) \quad (33)$$

where S is:

$$\begin{pmatrix} \omega_0 & \cdots & 0 \\ 0 & \omega_1 & \vdots \\ \vdots & \cdots & \omega_{18} \end{pmatrix} \quad (34)$$

Equation (33) is the workhorse for MRT method. To implement the MRT method, we need to determine two things:

1-The matrix M and the inverse of it.

2-The matrix S which is the relaxation time.

The matrix M can be calculated from the Hermite polynomial where M_i^j is equal to H_i^n:

IV. MRT IN D2Q9

Regarding the D2Q9 model in the context of MRT, the M matrix is as follows:

$$\begin{pmatrix} 1 & 1 & 1 & 1 & 1 & 1 & 1 & 1 & 1 \\ -4 & -1 & -1 & -1 & -1 & 2 & 2 & 2 & 2 \\ 4 & -2 & -2 & -2 & -2 & 1 & 1 & 1 & 1 \\ 0 & 1 & 0 & -1 & 0 & 1 & -1 & -1 & 1 \\ 0 & -2 & 0 & 2 & 0 & 1 & -1 & -1 & 1 \\ 0 & 0 & 1 & 0 & -1 & 1 & 1 & -1 & -1 \\ 0 & 0 & -2 & 0 & 2 & 1 & 1 & -1 & -1 \\ 0 & 1 & -1 & 1 & -1 & 0 & 0 & 0 & 0 \\ 0 & 0 & 0 & 0 & 0 & 1 & -1 & 1 & -1 \end{pmatrix} \quad (35)$$

Regarding the D2Q9 model in the context of MRT, the M^{-1} matrix is as follows:

$$\begin{pmatrix} 1/9 & -1/9 & 1/9 & 0 & 0 & 0 & 0 & 0 & 0 \\ 1/9 & -1/36 & -1/18 & 1/6 & -1/6 & 0 & 0 & 1/4 & 0 \\ 1/9 & -1/36 & -1/18 & 0 & 0 & 1/6 & -1/6 & -1/4 & 0 \\ 1/9 & -1/36 & -1/18 & -1/6 & 1/6 & 0 & 0 & 1/4 & 0 \\ 1/9 & -1/36 & -1/18 & 0 & 0 & -1/6 & 1/6 & -1/4 & 0 \\ 1/9 & 1/18 & 1/36 & 1/6 & 1/12 & 1/6 & 1/12 & 0 & 1/4 \\ 1/9 & 1/18 & 1/36 & -1/6 & -1/12 & 1/6 & 1/12 & 0 & -1/4 \\ 1/9 & 1/18 & 1/36 & -1/6 & -1/12 & -1/6 & -1/12 & 0 & 1/4 \\ 1/9 & 1/18 & 1/36 & 1/6 & 1/12 & -1/6 & -1/12 & 0 & -1/4 \end{pmatrix} \quad (36)$$

The moment vectors for vector m is as follows:

$$\boldsymbol{m} = (\rho, e, \varepsilon, j_x, q_x, j_y, q_y, P_{xx}, P_{xy})^T \quad (37)$$

The nine moments are defined as ρ being the fluid density, *e* is the energy, ε is related to the square of energy, j_x is the momentum of the fluid in the x-direction, q_x is moment related to flux in the x-direction, j_y is the momentum in the y-direction, q_y is the moment related to flux in the y-direction, P_{xx} is the moment related to the stress-rate tensor term in the xx-direction and P_{xy} is the stress-rate tensor term related to the xy-direction.

Moments ρ, j_x and j_y are the conserved moments, whereas e, ε, q_x, q_y, P_{xx}, P_{xy} are the non-conserved moments.

In the Lattice Boltzmann context, in order to calculate the macroscopic density and velocities, we perform an addition of the distribution functions for the density and an addition of the distribution functions multiplied by the velocity directions at each Lattice Boltzmann node, as follows:

$$\rho = \sum_i f_i \quad (38)$$

$$\boldsymbol{j} = \rho\mathbf{u} = \sum_i f_i \boldsymbol{c_i} \quad (39)$$

The equilibriums for the above 9 moments are as follows:

$$m_0^{eq} = \rho \quad (40)$$

$$m_1^{eq} = -2\rho + 3(j_x^2 + j_y^2) \quad (41)$$

$$m_2^{eq} = \rho - 3(j_x^2 + j_y^2) \quad (42)$$

$$m_3^{eq} = j_x \quad (43)$$

$$m_4^{eq} = -j_x \quad (44)$$

$$m_5^{eq} = j_y \quad (45)$$

$$m_6^{eq} = -j_y \quad (46)$$

$$m_7^{eq} = j_x^2 - j_y^2 \quad (47)$$

$$m_8^{eq} = j_x j_y \quad (48)$$

and the momentums in the x and y-directions are defined as:

$$j_x = \rho u_x \quad (49)$$

$$j_y = \rho u_y \quad (50)$$

The nine-velocity directions in two-dimensions are given as follows:

$$c = \begin{pmatrix} 0 & 1 & 0 & -1 & 0 & 1 & -1 & -1 & 1 \\ 0 & 0 & 1 & 0 & -1 & 1 & 1 & -1 & -1 \end{pmatrix} \quad (51)$$

The weights for all nine directions are as follows:

$$(4/9 \quad 1/9 \quad 1/9 \quad 1/9 \quad 1/9 \quad 1/36 \quad 1/36 \quad 1/36 \quad 1/36) \quad (52)$$

V. Flow Past a Cylinder Using the BGK

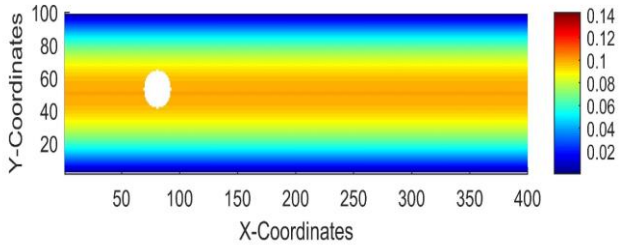

Fig. 1 Speed plot for the Poiseuille lid driven cavity flow using LB-BGK with uMax = 0.1 ms-1 at 0 time steps.

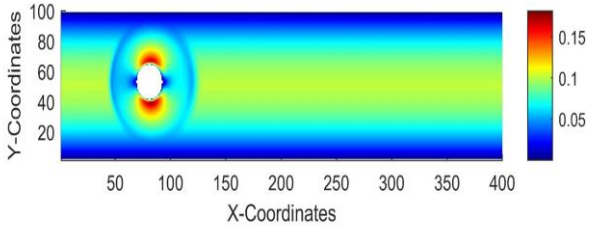

Fig. 2 Speed plot for the Poiseuille lid driven cavity flow using LB-BGK with uMax = 0.1 ms^{-1} at 50 time steps.

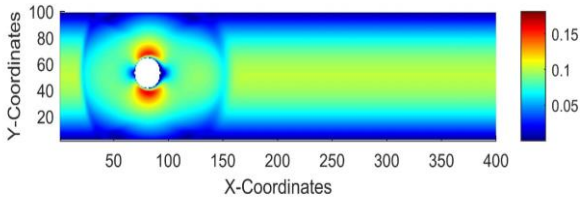

Fig. 3 Speed plot for the Poiseuille lid driven cavity flow using LB-BGK with uMax = 0.1 ms^{-1} at 100 time steps.

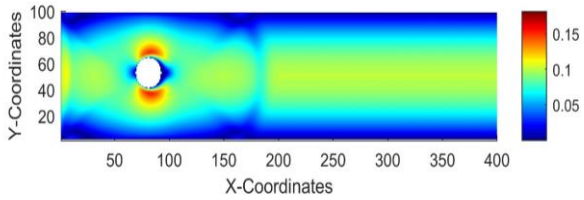

Fig. 4 Speed plot for the Poiseuille lid driven cavity flow using LB-BGK with uMax = 0.1 ms^{-1} at 150 time steps.

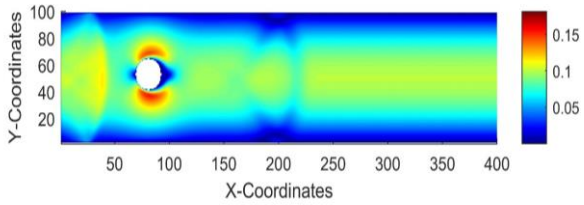

Fig. 5 Speed plot for the Poiseuille lid driven cavity flow using LB-BGK with uMax = 0.1 ms^{-1} at 200 time steps.

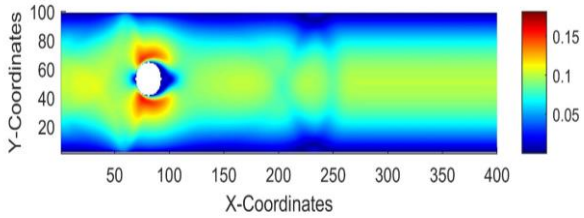

Fig. 6 Speed plot for the Poiseuille lid driven cavity flow using LB-BGK with uMax = 0.1 ms^{-1} at 250 time steps.

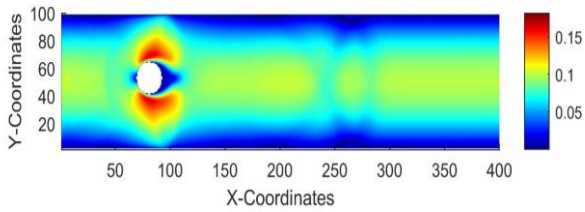

Fig. 7 Speed plot for the Poiseuille lid driven cavity flow using LB-BGK with uMax = 0.1 ms^{-1} at 300 time steps.

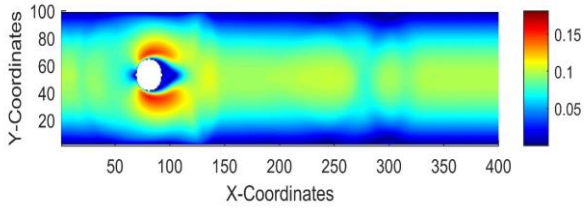

Fig. 8 Speed plot for the Poiseuille lid driven cavity flow using LB-BGK with uMax = 0.1 ms^{-1} at 350 time steps.

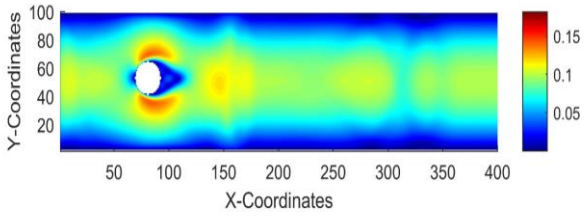

Fig. 9 Speed plot for the Poiseuille lid driven cavity flow using LB-BGK with uMax = 0.1 ms^{-1} at 400 time steps.

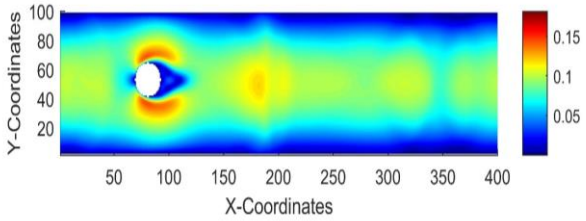

Fig. 10 Speed plot for the Poiseuille lid driven cavity flow using LB-BGK with uMax = 0.1 ms^{-1} at 450 time steps

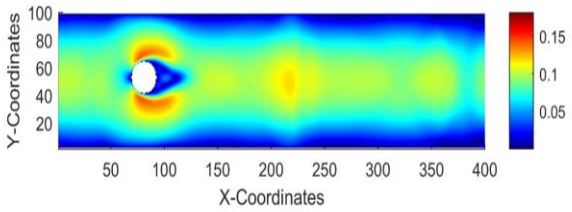

Fig. 11 Speed plot for the Poiseuille lid driven cavity flow using LB-BGK with uMax = 0.1 ms^{-1} at 500 time steps.

For the above simulation, the following parameters were used. The Reynolds number was set to 100 and the number of points in x and y-directions were set to lx=ly=400. The maximum velocity of the Poiseuille inflow was set to uMax=0.1 ms^{-1}. The radius of the cylinder was r = ly / 10.0 + 1.0 and the kinematic viscosity alpha = uMax * 2.0 * r / Re. The equilibrium relaxation frequency ω was calculated by ω = 1.0 / (3.0 * alpha + 0.5) and the equilibrium relaxation time τ was the inverse of ω. In this implementation, we have used the single relaxation BGK method.
Below we provide a detail flow chart of the steps necessary to conduct a LB-BGK simulation.

LB-BGK Solution Flow Chart

1. Define number of points in x and y direction
2. Define the lattice to use such as D2Q9
3. Create the x and y lattice mesh point coordinates
4. Define the weights, velocities of each x and y-direction, as well as the opposite direction vectors
5. Initialize macroscopic quantities such as densities at value rho and velocities
6. Set uMax of the inflow and rho=1.0
7. Set dx, dy and dt to 1 in lattice units
8. Create a boundary condition for the inlet boundary and identify lattice mesh points on the inlet
9. Create a boundary condition for the outlet boundary and identify lattice mesh points on the inlet
10. Create a boundary condition for the top and bottom boundaries to apply no-slip boundary condition and identify lattice mesh points and mask them
11. Define Reynolds number Re=rho*u_0*L/alpha where alpha is viscosity and L is length of the cavity
12. Calculate equilibrium relaxation frequency: ω = 1.0 / (3.0 * alpha + 0.5);
13. Calculate equilibrium relaxation time: τ = 1.0 / ω;
14. Mask the boundary of the circle by setting position of the center of mass of the cylinder: obst_x = lx / 5.0 + 1.0 and obst_y = ly / 2.0 + 3.0
15. Define number of times steps
16. Initialize conserved variables rho and **u**
17. Apply initial conditions for velocity in x-direction at u_0 at lid
18. Start the time loop
19. Calculate macroscopic variables
20. Perform collision
21. Perform streaming
22. Apply bounce back on west, east and south boundaries for no-slip boundary conditions
23. Boundary condition on the lid needs treatment by applying rules on the distribution functions to obey mass and momentum conservation, as well as equal non-equilibrium moments between opposite directions on the boundary
24. Calculate the macroscopic density
25. Calculate the macroscopic momentums
26. Divide macroscopic momentums by macroscopic densities to find macroscopic velocities
27. End time loop

VI. LID DRIVEN CAVITY FLOW USING THE MRT

Here we show the results for the well-known lid driven cavity flow in two-dimensions using the LB-MRT model.

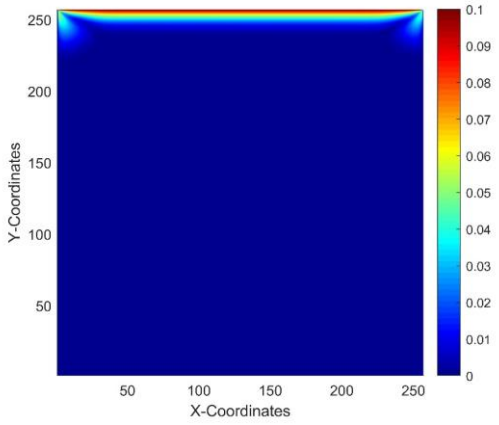

Fig. 12 Speed plot for the lid driven cavity flow using LB-MRT with u_0 = 0.1 ms^{-1} at 50 time steps.

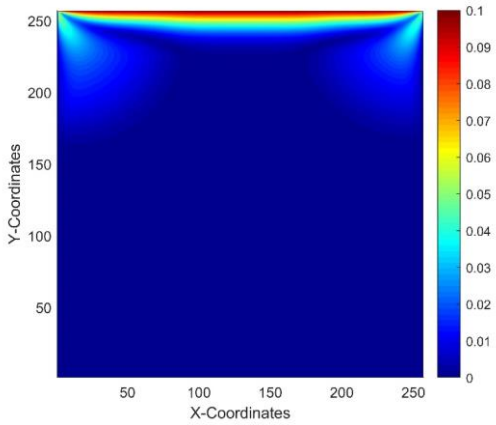

Fig. 13 Speed plot for the lid driven cavity flow using LB-MRT with $u_0 = 0.1\ ms^{-1}$ at 100 time steps.

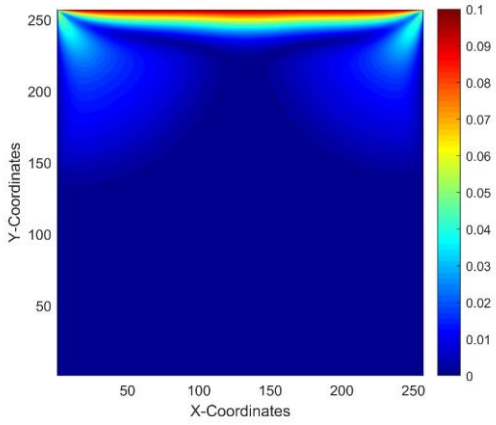

Fig. 14 Speed plot for the lid driven cavity flow using LB-MRT with $u_0 = 0.1\ ms^{-1}$ at 200 time steps.

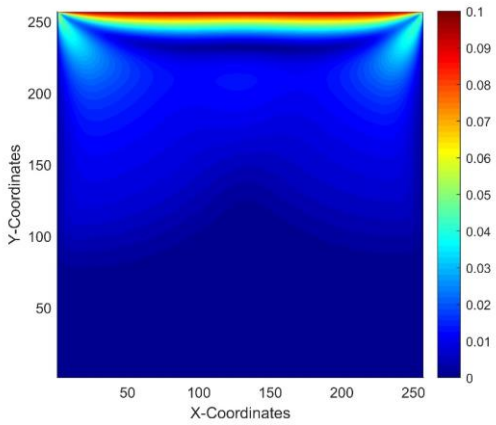

Fig. 15 Speed plot for the lid driven cavity flow using LB-MRT with $u_0 = 0.1\ ms^{-1}$ at 300 time steps.

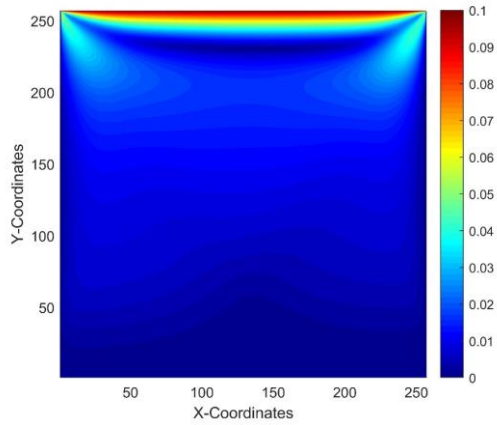

Fig. 16 Speed plot for the lid driven cavity flow using LB-MRT with $u_0 = 0.1\ ms^{-1}$ at 400 time steps.

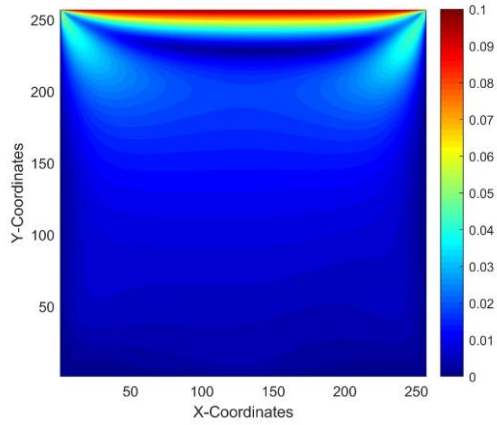

Fig. 17 Speed plot for the lid driven cavity flow using LB-MRT with $u_0 = 0.1\ ms^{-1}$ at 500 time steps.

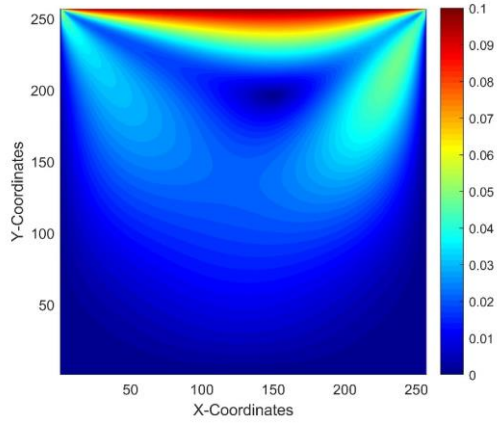

Fig. 18 Speed plot for the lid driven cavity flow using LB-MRT with $u_0 = 0.1\ ms^{-1}$ at 1,000 time steps.

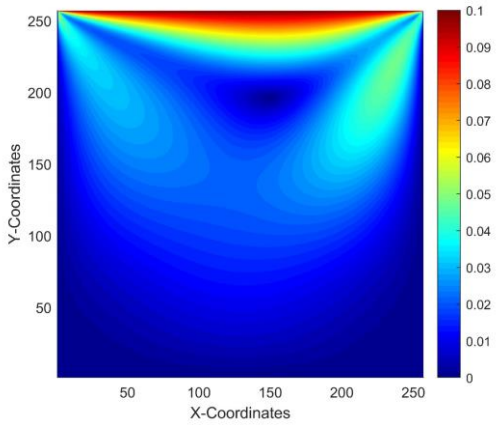

Fig. 19 Speed plot for the lid driven cavity flow using LB-MRT with u_0 = 0.1 ms^{-1} at 2,000 time steps.

For the above simulation, the following parameters were used. The Reynolds number was set to 500 and the number of points in x and y-directions were set to 256. The velocity of the lid was set to 0.1 ms^{-1} and the kinematic viscosity was calculated from Re=rho*u0*L/alpha, where L = 1. The equilibrium relaxation frequency ω was calculated by ω = 1.0 / (3.0 * alpha + 0.5) and the equilibrium relaxation time τ was the inverse of ω. To achieve stability, the diagonal relaxation matrix S was populated with τ.

LB-MRT Solution Flow Chart

1. Define number of points in x and y direction
2. Define the lattice to use such as D2Q9
3. Create the x and y lattice mesh points
4. Define the weights, velocities of each x and y-direction, as well as the opposite direction vectors
5. Initialize macroscopic quantities such as densities at value rho and velocities at 0, M and M^{-1} matrices
6. Set u_o of the lid and rho=1.0
7. Set dx, dy and dt to 1 in lattice units
8. Create a boundary condition for the lid and identify lattice mesh points on the lid
9. Define Reynolds number Re=rho*u0*L/alpha where alpha is the viscosity and L is length of cavity
10. Calculate equilibrium relaxation frequency: ω = 1.0 / (3.0 * alpha + 0.5);
11. Calculate equilibrium relaxation time: τ = 1.0 / ω;
12. Define the diagonal matrix S (vector form) populated by relaxation parameters
13. Calculate the $M^{-1}S$
14. Define number of times steps
15. Initialize conserved variables rho and **u**
16. Apply initial conditions for velocity in x-direction at u0 at lid
17. Start the time loop
18. Calculate equilibrium moments m_{eq}
19. Calculate Moments m = Mf in all of the grid
20. Perform collision in the moment space i.e. calculate post-collision operator f* by $f^*=f-M^{-1}*S[m-m_{eq}]$
21. Perform streaming
22. Apply bounce back on west, east and south boundaries for no-slip boundary conditions
23. Boundary condition on the lid needs treatment by applying rules on the distribution functions to obey mass and momentum conservation, as well as equal non-equilibrium moments between opposite directions on the boundary
24. Calculate the macroscopic density
25. Calculate the macroscopic momentums
26. Divide macroscopic momentums by macroscopic densities to find macroscopic velocities
27. End time loop

VII. Conclusions

In this paper, we provide firstly the incentive towards using Lattice Boltzmann BGK and MRT method. Secondly, we conducted a literature review with recent work on the application of LB-MRT in the various fields of engineering and physics. Thereafter, we included analytically the derivation of the LB-MRT method and applied BGK in flow past a cylinder and MRT in lid driven cavity flow and demonstrated clearly the necessary steps in conducting such simulations with the use of flowcharts, with an attempt for this paper to be used as a reference in conducting LB-MRT simulations. Since the results were conducted on the GPUs (Tesla K80), it was found that utilizing the GPUs, one can produce results accurate and efficiently, with the potential to provide real live simulations, when simulated with faster GPU cards out there, such as the NVIDIA P100 or V100.

Acknowledgment

This work was co-funded by the European Regional Development Fund of the European Union and the Republic of Cyprus through the Research and Innovation Foundation (Project: CONCEPT-COVID/0420/0025).

References

[1] K. R. Tubbs and F. T.-C. Tsai, "Mrt-lattice Boltzmann model for multilayer shallow water flow," *Water,* vol. 11, no. 8, p. 1623, 2019.

[2] K. Sato and S. Koshimura, "Validation of the MRT-LBM for three-dimensional free-surface flows: an investigation of the weak compressibility in dam-break benchmarks," *Coastal Engineering Journal,* vol. 62, no. 1, pp. 53-68, 2020/01/02 2020.

[3] A. Purqon, "Accuracy and Numerical Stabilty Analysis of Lattice Boltzmann Method with Multiple Relaxation Time for Incompressible Flows," in *Journal of Physics: Conference Series*, 2017, vol. 877, no. 1, p. 012035: IOP Publishing.

[4] F. Yang, X. Shi, X. Guo, and Q. Sai, "MRT Lattice Boltzmann Schemes for High Reynolds Number Flow in Two-Dimensional Lid-Driven Semi-Circular Cavity," *Energy Procedia,* vol. 16, pp. 639-644, 2012/01/01/ 2012.

[5] K. BOUARNOUNA, A. BOUTRA, M. BENZEMA, M. El Ganaoui, and Y. K. BENKAHLA, "Simulation of Natural Convection in a horizontal channel with heat sources mounted with porous blocks by the lattice Boltzmann method (MRT-LBM)," in *MATEC Web of Conferences*, 2020, vol. 307, p. 01009: EDP Sciences.

[6] Z. Chai and B. Shi, "Multiple-relaxation-time lattice Boltzmann method for the Navier-Stokes and nonlinear convection-diffusion equations: Modeling, analysis, and elements," *Physical Review E,* vol. 102, no. 2, p. 023306, 2020.

[7] A. De Rosis, R. Huang, and C. Coreixas, "Universal formulation of central-moments-based lattice Boltzmann method with external forcing for the simulation of multiphysics phenomena," *Physics of Fluids,* vol. 31, no. 11, p. 117102, 2019.

[8] A. De Rosis and C. Coreixas, "Multiphysics flow simulations using D3Q19 lattice Boltzmann methods based on central moments," *Physics of Fluids,* vol. 32, no. 11, p. 117101, 2020.

[9] M. Razzaghian, M. Pourtousi, and A. N. Darus, "Simulation of flow in lid driven cavity by MRT and SRT," in *Proc. Int. Conf. on Mechanical and Robotics Engineering (ICMRE'2012), Phuket, Thailand*, 2012, pp. 94-97.

[10] K. H. Luo, L. Fei, and G. Wang, "A unified lattice Boltzmann model and application to multiphase flows," *Philosophical Transactions of the Royal Society A,* vol. 379, no. 2208, p. 20200397, 2021.

[11] L. Jahanshaloo and N. A. Che Sidik, "Numerical Simulation of High Reynolds Number Flow Structure in a Lid-Driven Cavity Using MRT-LES," in *Applied Mechanics and Materials*, 2014, vol. 554, pp. 665-669: Trans Tech Publ.

[12] S. Ammar, G. Pernaudat, and J.-Y. Trépanier, "A multiphase three-dimensional multi-relaxation time (MRT) lattice Boltzmann model with surface tension adjustment," *Journal of Computational Physics,* vol. 343, pp. 73-91, 2017.

APPENDIX

MRT IN D3Q15

M-Matrix

$$\begin{pmatrix} 1 & 1 & 1 & 1 & 1 & 1 & 1 & 1 & 1 & 1 & 1 & 1 & 1 & 1 & 1 \\ -2 & -1 & -1 & -1 & -1 & -1 & -1 & 1 & 1 & 1 & 1 & 1 & 1 & 1 & 1 \\ 16 & -4 & -4 & -4 & -4 & -4 & -4 & 1 & 1 & 1 & 1 & 1 & 1 & 1 & 1 \\ 0 & 1 & -1 & 0 & 0 & 0 & 0 & 1 & -1 & 1 & -1 & 1 & -1 & 1 & -1 \\ 0 & -4 & 4 & 0 & 0 & 0 & 0 & 1 & -1 & 1 & -1 & 1 & -1 & 1 & -1 \\ 0 & 0 & 0 & 1 & -1 & 0 & 0 & 1 & 1 & -1 & -1 & 1 & 1 & -1 & -1 \\ 0 & 0 & 0 & -4 & 4 & 0 & 0 & 1 & 1 & -1 & -1 & 1 & 1 & -1 & -1 \\ 0 & 0 & 0 & 0 & 0 & 1 & -1 & 1 & 1 & 1 & 1 & -1 & -1 & -1 & -1 \\ 0 & 0 & 0 & 0 & 0 & -4 & 4 & 1 & 1 & 1 & 1 & -1 & -1 & -1 & -1 \\ 0 & 2 & 2 & -1 & -1 & -1 & -1 & 0 & 0 & 0 & 0 & 0 & 0 & 0 & 0 \\ 0 & 0 & 0 & 1 & 1 & -1 & -1 & 0 & 0 & 0 & 0 & 0 & 0 & 0 & 0 \\ 0 & 0 & 0 & 0 & 0 & 0 & 0 & 1 & -1 & -1 & 1 & 1 & -1 & -1 & 1 \\ 0 & 0 & 0 & 0 & 0 & 0 & 0 & 1 & 1 & -1 & -1 & -1 & -1 & 1 & 1 \\ 0 & 0 & 0 & 0 & 0 & 0 & 0 & 1 & -1 & 1 & -1 & -1 & 1 & -1 & 1 \\ 0 & 0 & 0 & 0 & 0 & 0 & 0 & 1 & -1 & -1 & 1 & -1 & 1 & 1 & -1 \end{pmatrix} \quad (53)$$

M^{-1} Matrix

$$\begin{pmatrix}
1/15 & -1/9 & 2/45 & 0 & 0 & 0 & 0 & 0 & 0 & 0 & 0 & 0 & 0 & 0 & 0 \\
1/15 & -1/18 & -1/90 & 1/10 & -1/10 & 0 & 0 & 0 & 0 & 1/6 & 0 & 0 & 0 & 0 & 0 \\
1/15 & -1/18 & -1/90 & -1/10 & 1/10 & 0 & 0 & 0 & 0 & 1/6 & 0 & 0 & 0 & 0 & 0 \\
1/15 & -1/18 & -1/90 & 0 & 0 & 1/10 & -1/10 & 0 & 0 & -1/12 & 1/4 & 0 & 0 & 0 & 0 \\
1/15 & -1/18 & -1/90 & 0 & 0 & -1/10 & 1/10 & 0 & 0 & -1/12 & 1/4 & 0 & 0 & 0 & 0 \\
1/15 & -1/18 & -1/90 & 0 & 0 & 0 & 0 & 1/10 & -1/10 & -1/12 & -1/4 & 0 & 0 & 0 & 0 \\
1/15 & -1/18 & -1/90 & 0 & 0 & 0 & 0 & -1/10 & 1/10 & -1/12 & -1/4 & 0 & 0 & 0 & 0 \\
1/15 & 1/18 & 1/360 & 1/10 & 1/40 & 1/10 & 1/40 & 1/10 & 1/40 & 0 & 0 & 1/8 & 1/8 & 1/8 & 1/8 \\
1/15 & 1/18 & 1/360 & -1/10 & -1/40 & 1/10 & 1/40 & 1/10 & 1/40 & 0 & 0 & -1/8 & 1/8 & -1/8 & -1/8 \\
1/15 & 1/18 & 1/360 & 1/10 & 1/40 & -1/10 & -1/40 & 1/10 & 1/40 & 0 & 0 & -1/8 & -1/8 & 1/8 & -1/8 \\
1/15 & 1/18 & 1/360 & -1/10 & -1/40 & -1/10 & -1/40 & 1/10 & 1/40 & 0 & 0 & 1/8 & -1/8 & -1/8 & 1/8 \\
1/15 & 1/18 & 1/360 & 1/10 & 1/40 & 1/10 & 1/40 & -1/10 & -1/40 & 0 & 0 & 1/8 & -1/8 & -1/8 & -1/8 \\
1/15 & 1/18 & 1/360 & -1/10 & -1/40 & 1/10 & 1/40 & -1/10 & -1/40 & 0 & 0 & -1/8 & -1/8 & 1/8 & 1/8 \\
1/15 & 1/18 & 1/360 & 1/10 & 1/40 & -1/10 & -1/40 & -1/10 & -1/40 & 0 & 0 & -1/8 & 1/8 & -1/8 & 1/8 \\
1/15 & 1/18 & 1/360 & -1/10 & -1/40 & -1/10 & -1/40 & -1/10 & -1/40 & 0 & 0 & 1/8 & 1/8 & 1/8 & -1/8
\end{pmatrix} \quad (54)$$

MRT IN D3Q19

M-Matrix

$$\begin{pmatrix}
1 & 1 & 1 & 1 & 1 & 1 & 1 & 1 & 1 & 1 & 1 & 1 & 1 & 1 & 1 & 1 & 1 & 1 & 1 \\
-30 & -11 & -11 & -11 & -11 & -11 & -11 & 8 & 8 & 8 & 8 & 8 & 8 & 8 & 8 & 8 & 8 & 8 & 8 \\
12 & -4 & -4 & -4 & -4 & -4 & -4 & 1 & 1 & 1 & 1 & 1 & 1 & 1 & 1 & 1 & 1 & 1 & 1 \\
0 & 1 & -1 & 0 & 0 & 0 & 0 & 1 & -1 & 1 & -1 & 1 & -1 & 1 & -1 & 0 & 0 & 0 & 0 \\
0 & -4 & 4 & 0 & 0 & 0 & 0 & 1 & -1 & 1 & -1 & 1 & -1 & 1 & -1 & 0 & 0 & 0 & 0 \\
0 & 0 & 0 & 1 & -1 & 0 & 0 & 1 & 1 & -1 & -1 & 0 & 0 & 0 & 0 & 1 & -1 & 1 & -1 \\
0 & 0 & 0 & -4 & 4 & 0 & 0 & 1 & 1 & -1 & -1 & 0 & 0 & 0 & 0 & 1 & -1 & 1 & -`1 \\
0 & 0 & 0 & 0 & 0 & 1 & -1 & 0 & 0 & 0 & 0 & 1 & 1 & -1 & -1 & 1 & 1 & -1 & -1 \\
0 & 0 & 0 & 0 & 0 & -4 & 4 & 0 & 0 & 0 & 0 & 1 & 1 & -1 & -1 & 1 & 1 & -1 & -1 \\
0 & 2 & 2 & -1 & -1 & -1 & -1 & 1 & 1 & 1 & 1 & 1 & 1 & 1 & 1 & -2 & -2 & -2 & -2 \\
0 & -4 & 4 & 2 & 2 & 2 & 2 & 1 & 1 & 1 & 1 & 1 & 1 & 1 & 1 & -2 & -2 & -2 & -2 \\
0 & 0 & 0 & 1 & 1 & -1 & -1 & 1 & 1 & 1 & 1 & -1 & -1 & -1 & -1 & 0 & 0 & 0 & 0 \\
0 & 0 & 0 & -2 & -2 & 2 & 2 & 1 & 1 & 1 & 1 & -1 & -1 & -1 & -1 & 0 & 0 & 0 & 0 \\
0 & 0 & 0 & 0 & 0 & 0 & 0 & 1 & -1 & -1 & 1 & 0 & 0 & 0 & 0 & 0 & 0 & 0 & 0 \\
0 & 0 & 0 & 0 & 0 & 0 & 0 & 0 & 0 & 0 & 0 & 0 & 0 & 0 & 0 & 1 & -1 & -1 & 1 \\
0 & 0 & 0 & 0 & 0 & 0 & 0 & 0 & 0 & 0 & 0 & 1 & -1 & -1 & 1 & 0 & 0 & 0 & 0 \\
0 & 0 & 0 & 0 & 0 & 0 & 0 & 1 & 1 & 1 & -1 & -1 & 1 & -1 & 1 & 0 & 0 & 0 & 0 \\
0 & 0 & 0 & 0 & 0 & 0 & 0 & -1 & -1 & 1 & 1 & 0 & 0 & 0 & 0 & 1 & -1 & 1 & -1 \\
0 & 0 & 0 & 0 & 0 & 0 & 0 & 0 & 0 & 0 & 0 & 1 & 1 & -1 & -1 & -1 & -1 & 1 & 1
\end{pmatrix} \quad (55)$$

M^{-1} Matrix

$$\begin{pmatrix}
1/19 & -5/399 & 1/21 & 0 & 0 & 0 & 0 & 0 & 0 & 0 & 0 & 0 & 0 & 0 & 0 & 0 & 0 & 0 & 0 \\
1/19 & -11/2394 & -1/63 & 1/10 & -1/10 & 0 & 0 & 0 & 0 & 1/18 & -1/18 & 0 & 0 & 0 & 0 & 0 & 0 & 0 & 0 \\
1/19 & -11/2394 & -1/63 & -1/10 & 1/10 & 0 & 0 & 0 & 0 & 1/18 & -1/18 & 0 & 0 & 0 & 0 & 0 & 0 & 0 & 0 \\
1/19 & -11/2394 & -1/63 & 0 & 0 & 1/10 & -1/10 & 0 & 0 & -1/36 & 1/36 & 1/12 & -1/12 & 0 & 0 & 0 & 0 & 0 & 0 \\
1/19 & -11/2394 & -1/63 & 0 & 0 & 0 & 0 & 1/10 & -1/10 & -1/36 & 1/36 & 1/12 & -1/12 & 0 & 0 & 0 & 0 & 0 & 0 \\
1/19 & -11/2394 & -1/63 & 0 & 0 & 0 & 0 & -1/10 & 1/10 & -1/36 & 1/36 & -/12 & 1/12 & 0 & 0 & 0 & 0 & 0 & 0 \\
1/19 & -11/2394 & -1/63 & 0 & 0 & 0 & 0 & -1/10 & 1/10 & -1/36 & 1/36 & -1/12 & 1/12 & 0 & 0 & 0 & 0 & 0 & 0 \\
1/19 & 4/1197 & 1/252 & 1/10 & 1/40 & 1/10 & 1/40 & 0 & 0 & 1/36 & 1/72 & 1/12 & 1/24 & 1/4 & 0 & 0 & 1/8 & -1/8 & 0 \\
1/19 & 4/1197 & 1/252 & -1/10 & -1/40 & 1/10 & 1/40 & 0 & 0 & 1/36 & 1/72 & 1/12 & 1/24 & -1/4 & 0 & 0 & -1/8 & -1/8 & 0 \\
1/19 & 4/1197 & 1/252 & 1/10 & 1/40 & -1/10 & -1/40 & 0 & 0 & 1/36 & 1/72 & 1/12 & 1/24 & -1/4 & 0 & 0 & 1/8 & 1/8 & 0 \\
1/19 & 4/1197 & 1/252 & -1/10 & -1/40 & -1/10 & -1/40 & 0 & 0 & 1/36 & 1/72 & 1/12 & 1/24 & 1/40 & 0 & -1/8 & 1/8 & 1/8 & 0 \\
1/19 & 4/1197 & 1/252 & 1/10 & 1/40 & 0 & 0 & 1/10 & 1/40 & 1/36 & 1/72 & -1/12 & -1/24 & 0 & 0 & 1/4 & -1/8 & 0 & 1/8 \\
1/19 & 4/1197 & 1/252 & -1/10 & -1/40 & 0 & 0 & 1/10 & 1/40 & 1/36 & 1/72 & -1/12 & -1/24 & 0 & 0 & -1/4 & 1/8 & 0 & 1/8 \\
1/19 & 4/1197 & 1/252 & 1/10 & 1/40 & 0 & 0 & -1/10 & -1/40 & 1/36 & 1/72 & -1/12 & -1/24 & 0 & 0 & -1/4 & -1/8 & 0 & -1/8 \\
1/19 & 4/1197 & 1/252 & -1/10 & -1/40 & 0 & 0 & -1/10 & -1/40 & 1/36 & 1/72 & -1/12 & -1/24 & 0 & 0 & 1/41/8 & 0 & & -1/8 \\
1/19 & 4/1197 & 1/252 & 0 & 0 & 1/10 & 1/40 & 1/10 & 1/40 & -1/18 & -1/36 & 0 & 0 & 01/4 & 0 & 0 & 1/8 & & -1/8 \\
1/19 & 4/1197 & 1/252 & 0 & 0 & -1/10 & -1/40 & 1/10 & 1/40 & -1/18 & -1/36 & 0 & 0 & 0 & 1/4 & 0 & 0 & -1/8 & 1/8 \\
1/19 & 4/1197 & 1/252 & 0 & 0 & 1/10 & 1/40 & -1/10 & -1/40 & -1/18 & -1/36 & 0 & 0 & 0 & -1/4 & 0 & 0 & 1/8 & 1/8 \\
1/19 & 4/1197 & 1/252 & 0 & 0 & -1/10 & -1/40 & -1/10 & -1/40 & -1/18 & -1/36 & 0 & 0 & 0 & -1/4 & 0 & 0 & -1/8 &
\end{pmatrix} \quad (56)$$